On the Inference of the One-Particle Density Matrix from Position and Momentum-Space Form Factors*

Hartmut Schmider and Vedene H. Smith, Jr.
Department of Chemistry, Queen's University, Kingston K7L 3N6, Ontario, Canada

Wolf Weyrich
Fakultät für Chemie, Universität Konstanz, D-W-7750 Konstanz, Fed. Rep. of Germany

Z. Naturforsch. **48a**, 211–220 (1993); received June 3, 1992

A modification of a recently developed method for the least-squares reconstruction of a one-particle reduced density matrix from experimentally accessible expectation values is applied to the test systems of atomic beryllium and neon. The improvement of the resulting matrices through inclusion of electron correlation is demonstrated. Their quality is judged by comparison of the moments of the position and momentum densities and of the spherically averaged density matrix in a suitable representation.

Key words: Density matrix; Reconstruction; Least-squares fit; Beryllium; Neon.

1. Introduction

The first successful attempt to reconstruct an *N-representable* one-particle density matrix (ODM) from a set of corresponding expectation values was reported in 1969 by Clinton and co-workers [1]. Since then, various approaches to this problem have been undertaken, most of them using the charge density or directly related quantities such as coherent scattering factors $F(\boldsymbol{k})$ as fitting data [2–7]. Almost all of these approaches impose the necessary N-representability conditions on the ODM by restricting it to an *idempotent* sub-class of allowed matrices (for an exception see [6]). This restriction may be given up by treating the eigenvalues of the ODM as parameters to be determined [5, 8, 9]. The necessary conditions on the eigenvalues are known [10] to be simple bounds. Hermiticity of the ODM may be enforced by imposing orthonormality conditions on the eigenfunctions of the ODM, i.e. the natural (spin) orbitals. This rather general technique [5] may be used in a least-squares framework to obtain *bona fide* ODMs from a given set of one-particle expectation values.

In cases where *both* position and momentum-density related data are used, it appears that relaxation of the idempotency condition is needed to obtain a proper reproduction of the data [8, 9]. In this paper, we emphasise this point by applying the principle mentioned above to atomic-electron systems. We assess the quality of the ODMs that were obtained from fits to form factors in position and momentum space by direct comparison in a suitable representation.

2. Principle of Parametrization

The technique employed in this work is a modification of our previous method [5, 8, 9]. In the following we present a spin-traced treatment, i.e. all spin-functions have been traced out implicitly. The inclusion of spin functions is straightforward, if somewhat tedious. Hereafter, the acronym ODM refers to the spin-traced one-particle density matrix.

The eigenfunctions of the ODM, the natural orbitals $\phi_j(\boldsymbol{r})$, may be expanded in terms of a given basis set $\{\chi\}$ of dimension m. The expansion coefficients c_{ij}, together with the eigenvalues n_j (occupation numbers) characterize the ODM in its matrix representation $\mathbf{P}$,

$$\begin{aligned} \varrho(\boldsymbol{r}, \boldsymbol{r}') &= \sum_j n_j \, \phi_j(\boldsymbol{r}) \, \phi_j^*(\boldsymbol{r}') \,, \\ \phi_j(\boldsymbol{r}) &= \sum_i \chi_i(\boldsymbol{r}) \, c_{ij} \,, \\ \mathbf{C} = \{c_{ij}\}, \quad \mathbf{N} &= \{\delta_{ij} \, n_j\} \,, \quad \mathbf{P} = \mathbf{C}\mathbf{N}\mathbf{C}^\dagger \,. \end{aligned} \tag{1}$$

* Presented at the Sagamore X Conference on Charge, Spin and Momentum Densities, Konstanz, Fed. Rep. of Germany, September 1–7, 1991.

Reprint requests to Prof. Dr. Vedene H. Smith, Jr., Department of Chemistry, Queen's University, Kingston K7L 3N6, Ontario, Canada.

0932-0784 / 93 / 0100-0211 $ 01.30/0. – Please order a reprint rather than making your own copy.

The goal is to parametrize **P** in such a way, that the *N-representability* conditions on the ODM are fulfilled. The parameters may then be used in a least-squares fit to experimental data $\{A_k^{\text{obs}}\}$,

$$\mathscr{S} = \sum_k (A_k^{\text{obs}} - \langle A_k \rangle)^2 \times \omega_k ,$$

$$\langle A_k \rangle = \text{trace}(\mathbf{P}\mathbf{A}_k) . \tag{2}$$

$\mathscr{A}_k$ denotes the operator associated with expectation values $\langle A_k \rangle$, and $\mathbf{A}_k$ is its representation in the basis set $\{\chi\}$,

$$\mathbf{A}_k = \{A_{ij}^k\} ,$$

$$A_{ij}^k = \int \chi_i^* \, \mathscr{A}_k \, \chi_j \, \mathrm{d}\tau . \tag{3}$$

The ω_k's in (2) denote weights, which are usually chosen to be proportional to the inverse of the variance of the expectation value.

The first condition on the ODM is that, since the ODM is hermitian (or, in the case of real coefficients, real-symmetric), its eigenvectors must be normalized and orthogonal. In other words, the matrix of coefficients, **C**, of these functions must fulfil the condition

$$\mathbf{C}^\dagger \boldsymbol{\Delta} \mathbf{C} = \mathbf{1} , \tag{4}$$

where $\boldsymbol{\Delta}$ is the metric matrix of the employed basis set. If the basis set is orthonormal, $\boldsymbol{\Delta}$ is the unit matrix and **C** is unitary (real-orthogonal).

The second condition is that the eigenvalues of the ODM, i.e. the occupation numbers n_j, be bounded and normalized,

$$0 \le n_j \le 2 , \quad \sum_j n_j = N . \tag{5}$$

If spin is included, the upper bound for the occupation numbers is, of course, 1 rater than 2 as in the spin-free treatment. N is the number of particles.

If the total wave function is approximated by a *single* Slater determinant, i.e. if an independent-particle model is applied, the occupation numbers in (5) are either 0 (for "virtual orbitals"), 1 (for a singly occupied spin-orbital) or 2 (for a spin-free orbital in a "restricted" treatment of a singlet-system). This leads to

$$\mathbf{N}^2 = \lambda \mathbf{N} \tag{6}$$

or, equivalently in terms of **P**,

$$\mathbf{P}\boldsymbol{\Delta}\mathbf{P} = \lambda \mathbf{P} . \tag{7}$$

The factor λ has been introduced in order to distinguish between the spin-discriminating ($\lambda = 1$) and the spin-traced singlet ($\lambda = 2$) case. Condition (7) is the discrete formulation, in a non-orthogonal basis set, of the aforementioned *idempotency* of the ODM,

$$\int \varrho(\boldsymbol{r}, \boldsymbol{r}'') \, \varrho(\boldsymbol{r}'', \boldsymbol{r}') \, \mathrm{d}\boldsymbol{r}'' = \lambda \varrho(\boldsymbol{r}, \boldsymbol{r}') . \tag{8}$$

The first condition, (4), may be enforced in different ways. Its nature is non-linear. A possible parametrization is to write **C** as an *infinite* product of planar rotation or Jacobi matrices. This method has been used in our earlier studies [5, 8, 9]. It is very simple to implement and rapidly converging, especially if second derivatives, which have a very simple form, are employed in addition. However, the benefit of a well-defined set of parameters is lacking. We use here a modification of this method, which has been proposed first (in a different context) by Raffenetti and Ruedenberg [11]. **C** may be written as a *finite* product $\mathbf{C}_R$ of planar rotation matrices $\mathbf{R}_v$ and an initial-guess matrix $\mathbf{C}_0$ that fulfils condition (4):

$$\mathbf{C} = \mathbf{C}_0 \mathbf{C}_R , \quad \mathbf{C}_R = \prod_v \mathbf{R}_v . \tag{9}$$

The resulting **C** matrix also satisfies (4), since unitary transformations leave the orthonormality of the natural orbitals invariant. The product (9) extends over all off-diagonal elements of an $m \times m$ matrix (m is the number of basis functions) that connect non-degenerate orbitals. $\mathbf{C}_R$ may be interpreted as the coefficient matrix of the resulting orbitals in terms of the ones defined by the columns of $\mathbf{C}_0$. One may look at $\mathbf{C}_R$ as having the form of a "generalized Euler matrix", since it defines a rotation in a higher-dimensional space in terms of a finite product of planar (2-dimensional) rotations.

The second condition, (5), is easier to fulfil. It requires just $\mu + 1$ linear constraints (5); μ is the number of occupied natural orbitals. Since the density matrix is a linear function of the occupation numbers, we may employ a *linear least-squares fit with linear constraints* for this part of the problem. If we restrict ourselves to an independent-particle model, the occupation numbers are fixed altogether, and we obtain an *idempotent* ODM, (6)–(8).

For these two sets of parameters taken together, we have implemented an algorithm that employs standard least-squares methods in a nested manner. For each evaluation of **P**, a constrained linear least-squares fit in the occupation numbers is performed. This requires the solution only of a system of linear equations. The parameters in the "Euler matrix" $\mathbf{C}_R$ are determined by a conventional non-linear least-

squares technique. Gradients are calculated numerically, since the implicit linear least-squares procedure makes their analytical evaluation cumbersome, if not impossible. The required least-squares fits are performed employing the NAG Fortran Library [12]. In the following, we apply this algorithm to the atomic systems of beryllium and neon.

3. Applications to Atomic Systems

3.1. Beryllium

Beryllium is a small atomic system for which electron correlation plays a very important rôle. Previously we have treated this system with the aforementioned Jacobi-type reconstruction method [9] and compared our results with the ones obtained by other authors within an idempotent framework [2, 4]. In the present study we employed as our "exact" wave function a more recent and better one [13] that is the result of a systematic attempt to converge the electron density with high accuracy. This CI expansion was used to calculate "experimental" sets of equally spaced atomic scattering factors $F(k)$ (designated FK in the Tables) and reciprocal form factors (also called internally folded densities) $B(s)$ (BS in the Tables) [14]. The former is the Fourier-Bessel transform of the spherically averaged charge density $\varrho(r)$, whereas the latter has an equivalent relationship to the spherically averaged momentum density $\pi(p)$. The range of data was chosen somewhat arbitrarily to cover values of F and B that are larger than 1% of the peak value (Table 1). The weight factors were unity in all cases.

Table 1. Data sets used for the ODM least-squares fit to "exact" beryllium data [13].

Label	Number	Kind	Range	Spacing
FK	200	$F(k)$	$0.10-20.0\ a_0^{-1}$	$0.10\ a_0^{-1}$
BS	200	$B(s)$	$0.05-10.0\ a_0$	$0.05\ a_0$
BF	200	comb.	$0.20-20.0\ a_0^{-1}$	$0.20\ a_0^{-1}$
			$0.10-10.0\ a_0$	$0.10\ a_0$

The reconstruction was performed in three basis sets: the NHF basis of Clementi and Roetti (CR) [15], the equivalent basis of Clementi (C) [16] (which is very similar), and the double-zeta basis of Clementi and Roetti (DZ) [15]. If correlation is included, the basis set has to be augmented at least by p-type functions. We used one set of 2p and one set of 3p-functions with an orbital exponent of 1.1 in all three cases. The second basis set (C) was employed to allow for slight variations in the basis, since our CI-expansion (i.e. our "exact" wave function) includes the CR basis as a subset.

The initial and final values of the sum of deviation squares, $\mathscr{S}$, are given in Table 2. Note that, in the cases of the NHF basis sets CR and C, for the data sets with only one kind of data (FK or BS) no variation of occupation numbers was performed, since the improvement of the $\mathscr{S}$ values was satisfactory by employing only idempotent ODMs. The corresponding attempt on a combined data set (labelled BF), however, fails. The idempotent ODM for the BF set does not im-

Table 2. Beryllium residual deviations in terms of $\mathscr{S}$, the weighted sum of deviation squares. The correlated fits are supplemented by the resulting occupation numbers in the order 1s/2s/3s/2p.

Fit	Initial guess	Idempotent	2p-corr.	2p + 3s-corr.
FK-CR	1.1×10^{-2}	3.1×10^{-8}	–	–
BS-CR	9.8×10^{-1}	5.9×10^{-8}	–	–
BF-CR	4.9×10^{-1}	6.4×10^{-3}	4.2×10^{-7} 2.0000/1.8283/0.0000/0.1717	1.5×10^{-7} 2.0000/1.7979/0.0048/0.1973
FK-C	1.1×10^{-2}	3.3×10^{-8}	–	–
BS-C	9.8×10^{-1}	3.7×10^{-8}	–	–
BF-C	4.9×10^{-1}	6.3×10^{-3}	7.6×10^{-7} 2.0000/1.8279/0.0000/0.1721	
FK-DZ	1.3×10^{-2}	1.1×10^{-4}	2.4×10^{-6} 2.0000/1.4587/0.0000/0.5413	–
BS-DZ	9.7×10^{-1}	4.6×10^{-4}	2.3×10^{-5} 2.0000/1.7699/0.0000/0.2301	–
BF-DZ	4.9×10^{-1}	3.3×10^{-2}	1.5×10^{-4} 2.0000/1.8313/0.0000/0.1687	1.0×10^{-4} 2.0000/1.8348/0.0130/0.1522

Table 3. Expectation values $\langle r^q \rangle$ for the idempotent and the 2 p-correlated fits to combined data sets (**BF**) in beryllium.

	$\langle r^{-2} \rangle$	$\langle r^{-1} \rangle$	$\langle r^{1} \rangle$	$\langle r^{2} \rangle$	$\langle r^{3} \rangle$	$\langle r^{4} \rangle$	$\langle r^{10} \rangle$	$\langle r^{20} \rangle$
CR initial guess	57.625	8.4088	6.1288	17.319	63.149	270.62	1.7859×10^{7}	6.6384×10^{17}
CR idempotent	58.893	8.4561	5.9571	16.617	63.394	308.24	9.5026×10^{7}	1.7666×10^{19}
CR 2p-corr.	57.619	8.4295	5.9786	16.291	57.039	233.80	1.1202×10^{7}	2.4103×10^{17}
C initial guess	57.625	8.4088	6.1289	17.320	63.164	270.76	1.7922×10^{7}	6.6896×10^{17}
C idempotent	59.014	8.4599	5.9537	16.616	63.725	314.17	1.1727×10^{8}	3.0718×10^{19}
C 2p-corr.	57.622	8.4260	5.9792	16.296	57.081	234.08	1.1115×10^{7}	2.0302×10^{17}
DZ initial guess	57.558	8.4084	6.1325	17.320	63.068	270.37	2.4615×10^{7}	1.0066×10^{19}
DZ idempotent	56.922	8.4350	5.8129	15.238	50.941	197.29	6.4569×10^{6}	2.5118×10^{18}
DZ 2p-corr.	57.516	8.4244	5.9772	16.256	56.672	230.81	1.2157×10^{7}	2.4803×10^{18}
CI "exact"	57.588	8.4254	5.9776	16.280	56.951	233.13	1.0979×10^{7}	2.1430×10^{17}

prove $\mathscr{S}$ convincingly. We therefore introduced correlation from the 2 s-orbital into the 2 p. As expected, the reproduction of the data becomes better by several orders of magnitude. Further inclusion of a 3 s-orbital yields (in this admittedly favourable case) additional improvement. Attempts to increase the number of partly occupied NOs even further failed, since the number of parameters became too large.

For the DZ basis set, all residual deviations are considerably larger than in the NHF cases. This is easy to understand, since the reproduction of salient features of densities is surely not a matter easily achieved with four s-type basis functions and fixed exponents. Correlation improves the picture for both "pure" data sets by more than an order of magnitude. A 3 s natural orbital could not be populated in these cases. For the combined set, the reproduction by idempotent ODMs is particularly poor. Correlation into 2 p lowers $\mathscr{S}$ by more than two orders of magnitude, and the additional occupation of a 3 s-orbital improves the reproduction even further. The low deviations of the NHF fits cannot be reached.

Table 2 gives also the resulting occupation numbers of the ODMs. For the combined fits they are relatively close to the ones of the "exact" solution (1.9962, 1.8208, 0.0037 and 0.1749 for 1 s, 2 s, 3 s, and 2 p, respectively), but in the "pure" fits employing the DZ basis there is a tendency to overestimate the degree of correlation. The closest reproduction is obtained with the 2 p-only correlated fits in the CR and C basis sets.

The question of how far these results reproduce the "exact" function may be investigated by means of charge and momentum densities or their moments $\langle r^q \rangle$ and $\langle p^q \rangle$. Tables 3 and 4 collect these expectation values for various values of q. Only *combined* fits are considered. Though fits to only one kind of data are sometimes able to improve the reproduction in the *complementary* space, the improvement is not very strong (see for example [9] and our treatment of neon in Section 3.2). We focus here on the advantage of relaxing the idempotency restriction.

Table 4. Expectation values $\langle p^q \rangle$ for the idempotent and the 2 p-correlated fits to combined data sets (**BF**) in beryllium.

	$\langle p^{-2} \rangle$	$\langle p^{-1} \rangle$	$\langle p^{1} \rangle$	$\langle p^{2} \rangle$	$\langle p^{3} \rangle$	$\langle p^{4} \rangle$
CR initial guess	25.290	6.3182	7.4342	29.146	185.59	2161.0
CR idempotent	22.456	5.9339	7.6410	31.154	217.27	2970.1
CR 2p-corr.	21.959	5.9091	7.5294	29.303	186.22	2172.6
C initial guess	25.298	6.3188	7.4342	29.146	185.59	2161.1
C idempotent	22.516	5.9374	7.6362	31.132	217.54	2987.5
C 2p-corr.	21.953	5.9088	7.5297	29.307	186.29	2174.4
DZ initial guess	25.448	6.3261	7.4321	29.146	185.26	2139.9
DZ idempotent	21.342	5.8932	7.5206	29.153	182.71	2076.9
DZ 2p-corr.	21.978	5.9097	7.5277	29.274	185.40	2141.1
CI "exact"	21.959	5.9091	7.5304	29.314	186.21	2163.6

As may be seen from the Tables, the *correlated* fits (at least in the CR and C basis sets) are generally able to yield a better reproduction than the NHF initial guess for all expectation values with the exception of the $\langle r^{-2} \rangle$ and the $\langle p^4 \rangle$ values. These describe the fast electrons close to the nucleus, in other words mainly the "inner" core region. Both the large-p and the small-r regions are difficult to describe with high accuracy. They are connected to the cusp at the nucleus [17] and the asymptotic behaviour of the momentum density [18]. This problem could be overcome by either fixing the core region with additional constraints (cusp-condition) [19], by employing an unreasonably

high density of points in $B(s)$ for small s ($\langle p^4 \rangle$ is the third term in the Taylor expansion of $B(s)$ near the origin [20]) or by using a set of $F(k)$ values that extends to very high k (which is equivalent to employing the behaviour of the derivatives of ϱ near the nucleus). Note that for all other expectation values the improvement is considerable. Some of them ($\langle p^{-1} \rangle$ and $\langle p^{-2} \rangle$) are "exact" to five significant figures. The "valence" moments (negative powers of p and large powers of r) are especially well described.

The *idempotent* fits are much less convincing, as already reflected by the comparably high residual values of $\mathscr{S}$. Correlation appears to be necessary to describe the densities in both spaces sufficiently. The DZ fits show analogous tendencies, but are generally less accurate. Their lower flexibility, however, keeps the $\langle r^{-2} \rangle$ and $\langle p^4 \rangle$ values from "breaking out". As a consequence, even these values are improved with respect to the initial guess in the correlated case.

In order to investigate the total reproduction of the ODM in more detail, we also present residual deviations in a spherically averaged ODM-representation [9, 21] that is given in terms of sum and difference coordinates [22],

$$\boldsymbol{R} = \frac{\boldsymbol{r} + \boldsymbol{r}'}{2}, \quad \boldsymbol{s} = \boldsymbol{r}' - \boldsymbol{r}. \tag{10}$$

The ODM is then represented in these new coordinates, and the spherical average is obtained over the orientations of $\boldsymbol{R}$ and $\boldsymbol{s}$. The ODM is additionally weighted by $4\pi R^2$ in order to account for the proper volume element in $\boldsymbol{R}$,

$$\begin{aligned} \varrho'(\boldsymbol{R}, \boldsymbol{s}) &= \varrho(\boldsymbol{r}, \boldsymbol{r}'), \\ \varrho^{\Omega}(R, s) &= (4\pi)^{-1} R^2 \int \varrho'(\boldsymbol{R}, \boldsymbol{s}) \, \mathrm{d}\Omega_R \, \mathrm{d}\Omega_s . \end{aligned} \tag{11}$$

This way of representing the ODM has the advantage that its value at $s = 0$ equals the radial charge density $D(R)$, and an integral over R at a fixed value of s gives the reciprocal form factor $B(s)$,

$$\varrho^{\Omega}(R, 0) = D(R), \quad \int \varrho^{\Omega}(R, s) \, \mathrm{d}R = B(s). \tag{12}$$

We have considered only the combined fits in Figures 3–6. The results in the Clementi basis are naturally quite similar to the ones in the CR basis. We have therefore restricted ourselves to the latter and the DZ basis set. Figure 1 shows ϱ^{Ω} for the beryllium atom in the original CI description. Obvious features are two peaks extending from the R-axis into the ODM. They may easily be associated with K and L-shell contributions. At the bottom we have plotted a cut through ϱ^{Ω} with $s = 0$, i.e. $D(R)$, and on the left-hand side the integral over ϱ^{Ω} parallel to the R-axis, i.e. $B(s)$. The two peaks are well resolved in the radial charge density, and since they differ in their extension into the off-diagonal region, they give (on integration) rise to a noticeable change in the slope of $B(s)$.

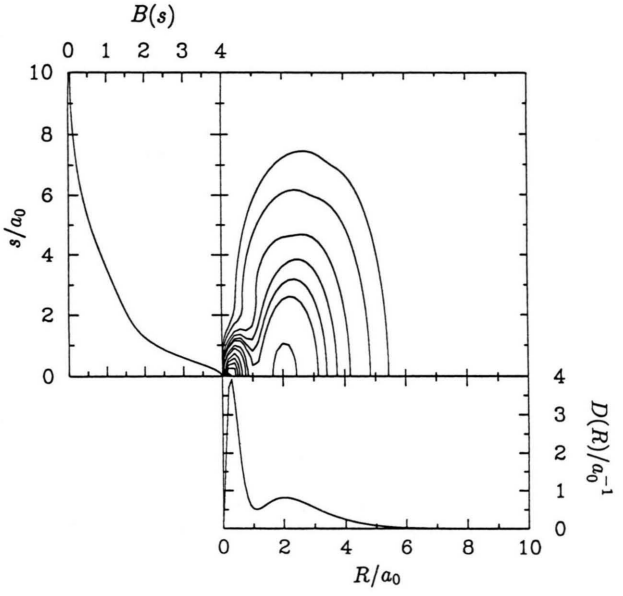

Fig. 1. Spherically averaged ODM in the form of $\varrho^{\Omega}(R, s)$ for the CI function [13] of beryllium. To the left, the spherically averaged reciprocal form factor $B(s)$, which arises from integration over R, has been plotted. At the bottom, the radial charge density $D(R)$, which is a cut through ϱ^{Ω}, is depicted. The contour lines are 0.05, 0.1, 0.2, 0.3, 0.4, 0.5, 0.75, 1.0, 1.5, 2.0, 3.0 and 3.5 a_0^{-1}.

Figure 2 shows the deviation in ϱ^{Ω} for the (NHF) initial guess. It may be generally assessed that the independent-particle model overestimates the range of the valence part, which gives rise to a fairly large peak in the difference-ODM. The underestimation of the core region appears as a negative peak in $\Delta D(R)$ and $\Delta\varrho^{\Omega}$ around $R = 2a_0$.

An attempt to fit the ODM in the idempotent framework (Fig. 3) yields an interesting result: The overall deviations become considerably larger, rather than smaller. Especially the charge density is poorly represented by this fit. The reason becomes clear if one considers that the major contribution to the initial deviations (see Table 2) are due to $B(s)$. An idempotent fit will therefore first attempt to lower these deviations at the expense of the reproduction of the $F(k)$ values. This is achieved in our case by restructuring the off-

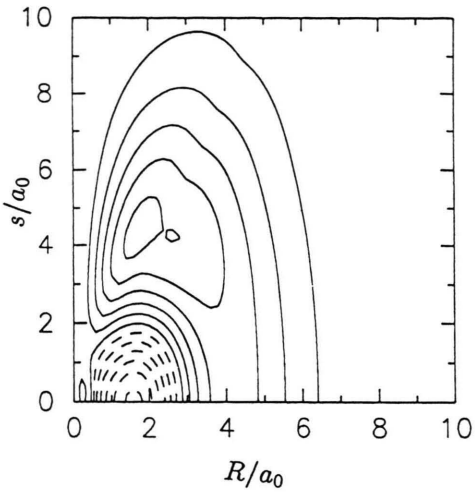

Fig. 2. Residual deviations in ϱ^{Ω} for the initial guess (NHF) [15] in beryllium. The reference is the CI calculation [13]. Non-negative contours are full, negative ones are dashed. The contour line spacing is 0.005 a_0^{-1}.

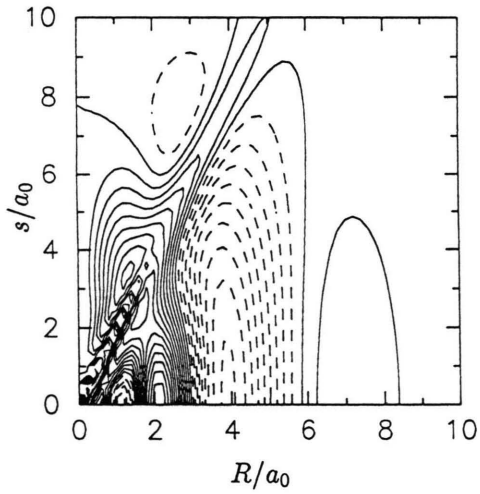

Fig. 3. Residual deviations in ϱ^{Ω} for the *idempotent* solution of the combined fit in the NHF basis [15] in beryllium. The reference is the CI calculation [13]. Non-negative contours are full, negative ones are dashed. The contour line spacing is 0.005 a_0^{-1}.

diagonal regions of the ODM ($s > 0$) in such a way that positive and negative deviations cancel partially on integration, thereby lowering the deviation in $B(s)$. This phenomenon is less pronounced when the deviations of $F(k)$ are weighted more strongly (by choosing ω_k's in (2) different from 1). We were, on the other hand, not able to obtain correlated fits employing a weighting scheme of this sort.

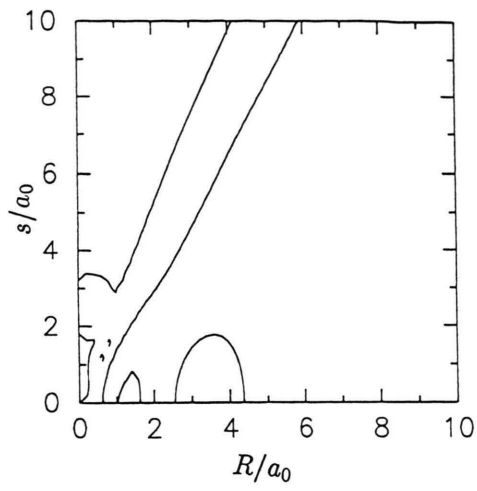

Fig. 4. Residual deviations in ϱ^{Ω} for the 2p-*correlated* solution of the combined fit in the NHF basis [15] in beryllium. The reference is the CI calculation [13]. Non-negative contours are full, negative ones are dashed. The contour line spacing is 0.005 a_0^{-1}.

On correlation, the residual deviations in ϱ^{Ω} reduce to a shallow valley along the "cusp line" $R = s/2$ and to some small oscillations along the R-axis (Figure 4). The additional flexibility allows the system to reproduce both position and momentum densities with reasonable accuracy. The resulting ODM resembles the "exact" one quite closely.

Figures 5 and 6 show the corresponding deviations (idempotent and 2p-correlated fits) in the DZ basis set. For the idempotent case, the overall deviations in ϱ^{Ω} are less pronounced than in the CR case, owing to the smaller flexibility of the basis set and the resulting smaller "overcompensation" effect discussed before. The correlated ODM deviates, of course, more strongly than the corresponding one in the CR basis set, which is clear when remembering that $\mathscr{S}$ is more than two orders of magnitude larger. There are still considerable oscillations left along R, but the overall reproduction of the ODM has improved much in comparison with the initial guess and the idempotent solution.

3.2. *Neon*

The ODM-fitting procedure was applied to the ten-electron system of neon. Since the neon atom is considerably more contracted than beryllium, we had to choose different ranges of data than in our first

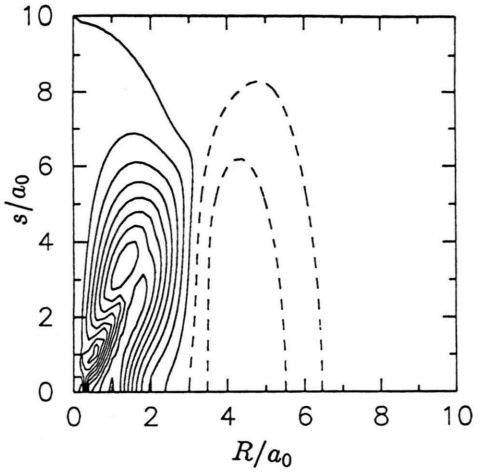

Fig. 5. Residual deviations in ϱ^{Ω} for the *idempotent* solution of the combined fit in the DZ basis [15] in beryllium. The reference is the CI calculation [13]. Non-negative contours are full, negative ones are dashed. The contour line spacing is 0.005 a_0^{-1}.

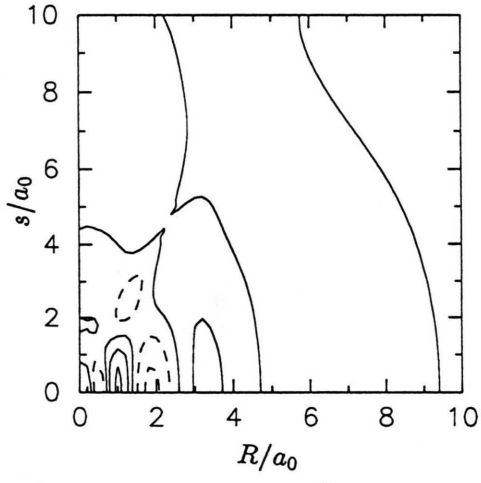

Fig. 6. Residual deviations in ϱ^{Ω} for the 2p-*correlated* solution of the combined fit in the DZ basis [15] in beryllium. The reference is the CI calculation [13]. Non-negative contours are full, negative ones are dashed. The contour line spacing is 0.005 a_0^{-1}.

Table 5. Data sets used for the ODM least-squares fit to "exact" neon data [23].

Label	Number	Kind	Range	Spacing
FK	200	$F(k)$	$0.200-40.0\,a_0^{-1}$	$0.200\,a_0^{-1}$
BS	200	$B(s)$	$0.025-5.0\,a_0$	$0.025\,a_0$
BF	200	comb.	$0.400-40.0\,a_0^{-1}$	$0.400\,a_0^{-1}$
			$0.050-5.0\,a_0$	$0.050\,a_0$

example. They are given in Table 5. The k-range has been doubled in order to cover all values larger than 1% of the peak, and the s range was halved in order to include major parts of the negative regions in $B(s)$. As "exact" data for fitting we have taken form-factor values obtained from a wave function by Bunge and Esquivel [23] that is given in an extension of the NHF basis set of Clementi and Roetti [15]. The fits were performed in the original (unextended) CR basis.

The resulting fits are listed in Table 6. The idempotency condition could be retained in both "pure" fits, since very low residuals were reached without including electron correlation (FK and BS). The combined fit, BF, yields an improvement in $\mathscr{S}$ of only a factor of five in the idempotent approximation. Introduction of correlation simultaneously from 2s and 2p into the 3s and 3p-states leads to such a high number of parameters (17 angles and 4 occupation numbers) that no convergence could be reached. We have, however, obtained two fairly low lying solutions, one with an additional occupied 3p-shell (the occupation numbers of the 1s and the 2p are kept fixed) and one with a partially occupied 3s-orbital (only the 1s-occupation is kept fixed). Since the former shows the lower deviations, we focus in the following only on this solution.

From the moments of the position and momentum densities (Tables 7 and 8) we see that each of the "pure" fits improves mainly the reproduction of the corresponding density. Complementary expectation values (i.e. r-moments for $B(s)$ and p-moments for $F(k)$) are often poorer than the initial guess. Note that the $B(s)$-fit describes large-r (outer-valence) regions considerably better than the NHF function, and that the $F(k)$-fit produces a better $\langle p \rangle$ value. However, in order to get an overall improvement, one has to do a combined fit. Since the idempotent BF-fit shows such large residuals, only some expectation values (e.g. $\langle p^{-2} \rangle$ and $\langle r \rangle$) improve, whereas others (e.g. $\langle p^2 \rangle$ and $\langle r^{-1} \rangle$) become poorer. Finally, the 2p-correlated combined fit improves all values with the aforementioned exceptions of $\langle r^{-2} \rangle$ and $\langle p^4 \rangle$, which are, of course, very well described already in the Hartree-Fock initial guess.

The residual deviations in ϱ^{Ω} confirm the expected behaviour (Figs. 8–11). In order to obtain a general idea of the form of ϱ^{Ω} for neon, we have depicted the function in Figure 7. As for beryllium, $B(s)$ and $D(R)$ are plotted to the left and the bottom. Note that $B(s)$ becomes negative at $s \approx 3.5\,a_0$. Since the absolute

Table 6. Neon residual deviations in terms of $\mathscr{S}$, the weighted sum of deviation squares (all in CR [15] basis). For the correlated fits the occupation numbers are given in the order 1s/2s/3s/2p/3p.

Fit	Initial guess	Idempotent	3p-corr.	3s-corr.
FK	4.4×10^{-3}	1.6×10^{-8}	–	–
BS	3.7×10^{-2}	1.7×10^{-8}	–	–
BF	2.1×10^{-2}	4.0×10^{-3}	6.3×10^{-7} 2.0000/1.9604/0.0000/6.0000/0.0396	1.2×10^{-6} 2.0000/2.0000/0.0947/5.9053/0.0000

Table 7. Expectation values $\langle r^q \rangle$ for the fits in Table 6 (neon in CR [15] basis set).

	$\langle r^{-2} \rangle$	$\langle r^{-1} \rangle$	$\langle r^{1} \rangle$	$\langle r^{2} \rangle$	$\langle r^{3} \rangle$	$\langle r^{4} \rangle$	$\langle r^{10} \rangle$	$\langle r^{20} \rangle$
Initial guess	414.90	31.113	7.8916	9.3758	14.409	27.339	32327.	4.1167×10^{12}
FK idempotent	415.17	31.111	7.9354	9.5444	14.938	28.993	38616.	5.0984×10^{12}
BS idempotent	418.81	30.880	7.9642	9.4514	14.549	27.946	38910.	5.3240×10^{12}
BF idempotent	415.92	31.120	7.9258	9.5125	14.845	28.705	36986.	4.7828×10^{12}
BF 3p-corr.	415.11	31.111	7.9359	9.5478	14.955	29.067	39564.	5.3173×10^{12}
BF 3s-corr.	415.15	31.112	7.9355	9.5451	14.943	29.021	39141.	5.2250×10^{12}
CI "exact"	414.97	31.110	7.9354	9.5448	14.941	29.006	38798.	5.1364×10^{12}

Table 8. Expectation values $\langle p^q \rangle$ for the fits in Table 6 (neon in CR [15]).

	$\langle p^{-2} \rangle$	$\langle p^{-1} \rangle$	$\langle p^{1} \rangle$	$\langle p^{2} \rangle$	$\langle p^{3} \rangle$	$\langle p^{4} \rangle$
Init. guess	5.4795	5.4557	35.196	257.09	3584.3	9.8596×10^{4}
FK idemp.	5.2129	5.4061	35.227	259.15	3657.4	1.0179×10^{5}
BS idemp.	5.5518	5.4782	35.242	257.79	3594.7	9.9040×10^{4}
BF idemp.	5.5722	5.4805	35.331	260.84	3696.0	1.0415×10^{5}
BF 3p-corr.	5.5518	5.4782	35.241	257.79	3595.2	9.9090×10^{4}
BF 3s-corr.	5.5529	5.4783	35.245	257.89	3597.3	9.9109×10^{4}
CI "exact"	5.5527	5.4782	35.241	257.75	3591.5	9.8719×10^{4}

magnitude of the negative values never exceeds 0.02, the negative region is not visible on our scale.

Although the $F(k)$-fit (Fig. 9) reproduces ϱ^{Ω} along and near the R-axis very well, it shows systematic deviations in the off-diagonal region in the former of a positive and two negative peaks, which are grouped along the line $R = s/2$ in such a manner that they will not cancel upon R-integration and therefore create deviations in $B(s)$. Analogously, the $B(s)$-fit shows very large oscillations along the R-axis, which partly cancel upon integration but remain in the charge density. Note that in Fig. 10 we had to cut off the peaks

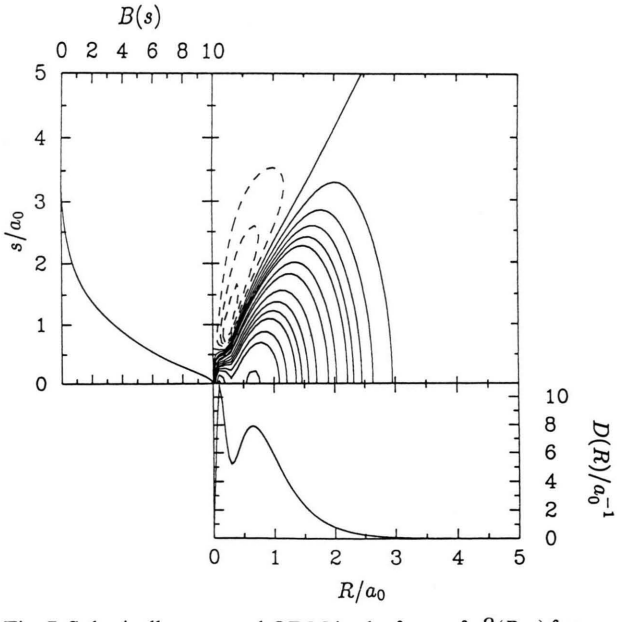

Fig. 7. Spherically averaged ODM in the form of $\varrho^{\Omega}(R, s)$ for the CI function [23] of neon. To the left, the spherically averaged reciprocal form factor $B(s)$, which arises from integration over R, has been plotted. Note that the negative region ($s > 3.5\ a_0$) is not visible in our scale. At the bottom, the radial charge density $D(R)$, which is a cut through ϱ^{Ω}, is depicted. The contour lines are -0.3, -0.2, -0.1, 0.0, 0.1, 0.2, 0.3, 0.4, 0.5, 0.75, 1.0, 1.5, 2.0, 2.5, 3.0, 4.0, 5.0, 7.5 and 10.0 a_0^{-1}. Non-negative countour lines are full, negative ones are dashed.

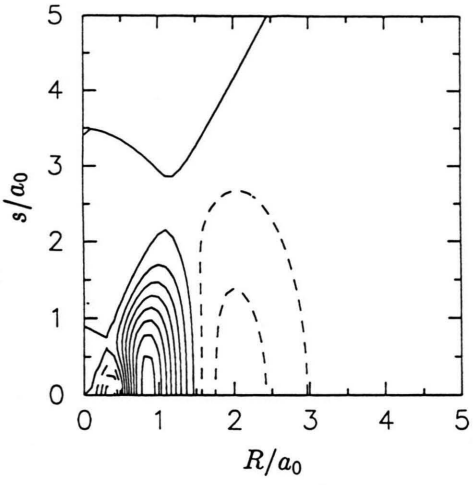

Fig. 8. Residual deviations in ϱ^{Ω} for the (NHF) [15] initial guess in neon. The reference is the CI calculation [23]. Non-negative contours are full, negative ones are dashed. The contour line spacing is 0.01 a_0^{-1}.

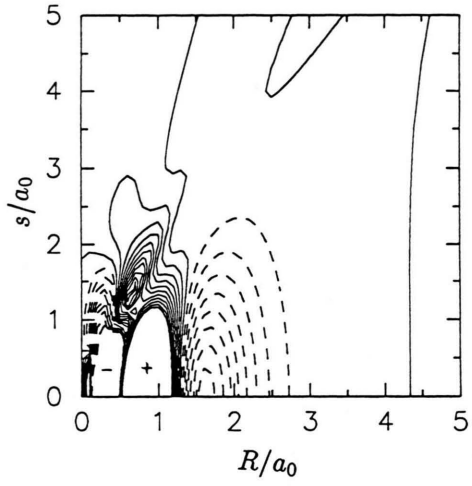

Fig. 10. Residual deviations in ϱ^{Ω} for the *idempotent* solution of the $B(s)$-fit in the NHF basis [15] in neon. The reference is the CI calculation [23]. Non-negative contours are full, negative ones are dashed. The areas in the low-s regions labelled with − and + are negative and positive peaks that have been cut off. The contour line spacing is 0.01 a_0^{-1}.

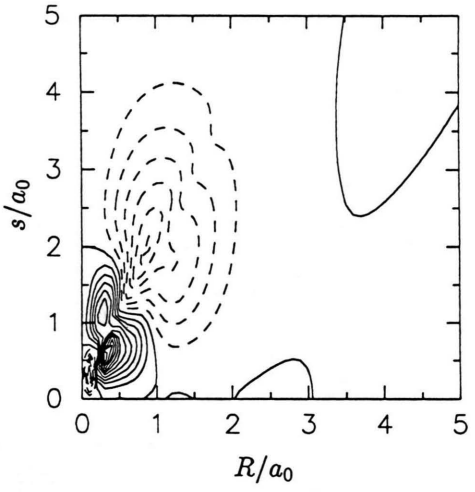

Fig. 9. Residual deviations in ϱ^{Ω} for the *idempotent* solution of the $F(k)$-fit in the NHF basis [15] in neon. The reference is the CI calculation [23]. Non-negative contours are full, negative ones are dashed. The contour line spacing is 0.01 a_0^{-1}.

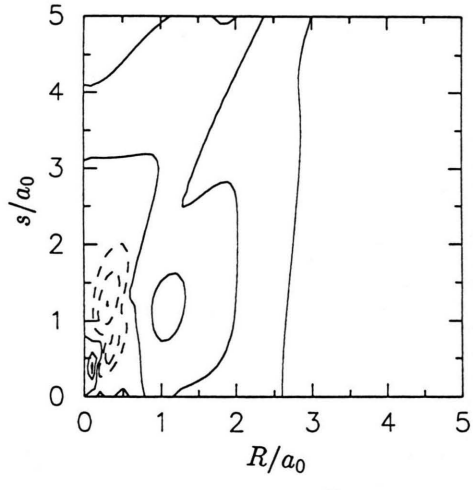

Fig. 11. Residual deviations in ϱ^{Ω} for the 2p-*correlated* solution of the *combined* fit in the NHF basis [15] in neon. The reference is the CI calculation [23]. Non-negative contours are full, negative ones are dashed. The contour line spacing is 0.01 a_0^{-1}.

to retain the contour spacing of 0.01 a_0^{-1}. They have been replaced by their sign (+ or −). The 2p-correlated fit to the combined data finally shows a considerably closer reproduction of the ODM in all regions (Figure 11). The remaining deviations partly cancel on integration (to give $B(s)$) and are to some extent due to the aforementioned problems of describing the regions near the nucleus accurately.

4. Conclusions and Outlook

It is possible to find ODMs that reproduce given sets of (possible experimental) expectation values with a high degree of accuracy. Given a fairly complete basis set, this reproduction may be achieved with idempotent ODMs, i.e. in the framework of an independent-particel model.

Problems are encountered whenever data sets of both position and momentum-space quantities have to be fitted. In these cases, inclusion of electron correlation (and the resulting increase in the number of parameters) become necessary if good agreement with the data is required. For small basis sets, the reproduction is, of course, less accurate. Electron correlation improves the fits considerably and may therefore be employed even for "pure" position or momentum data sets.

As the number of parameters increases, the problem of multiple minima and hence of initial-guess dependence becomes important. This problem may be overcome, since *ab-initio* calculations supply an obvious starting point for reconstructions of this kind. As has been pointed out [24–26], in the majority of cases there is no (practically) unique solution of the density-matrix reconstruction problem, even if both position and momentum densities are well-defined. We are, however, able to obtain solutions that comply with the original data and show only small deviations over wide regions of the ODM.

In practical cases, where the number and quality [27] of available data is restricted, judicious choices have to be made in order to restrict the number of required parameters [28]. The initial guess is in these cases of crucial importance. The method employed in this work offers the unique opportunity of using quantum-mechanical calculations as initial guesses and modifying them in a controlled way to reproduce given data.

Acknowledgements

We would like to thank Rodolfo O. Esquivel for the atomic CI wave functions used in this work. The financial support from NSERCC (Natural Science and Engineering Research Council of Canada) and the Fonds der Chemischen Industrie is gratefully acknowledged. One of us (H.S.) held an R. S. McLaughlin Fellowship at the time when this research was done.

[1] W. L. Clinton, J. Nakhleh, and F. Wunderlich, Phys. Rev. **177,** 1 (1969).
[2] C. Frishberg and L. J. Massa, Phys. Rev. B **24,** 7018 (1981).
[3] L. Massa, M. Goldberg, C. Frishberg, R. F. Boehme, and S. J. LaPlaca, Phys. Rev. Lett. **55,** 622 (1985).
[4] C. Frishberg, Int. J. Quantum Chem. **30,** 1 (1986).
[5] H. Schmider, Diplomarbeit, Universität Konstanz, 1986.
[6] K. Tanaka, Acta Cryst. A **44,** 1002 (1988).
[7] Y. V. Aleksandrov, V. G. Tsirel'son, I. M. Reznik, and R. P. Ozerov, phys. stat. sol. (b) **155,** 201 (1989).
[8] H. Schmider, V. H. Smith, Jr., and W. Weyrich, Trans. Amer. Cryst. Assoc. **26,** 125 (1990).
[9] H. Schmider, V. H. Smith, Jr., and W. Weyrich, J. Chem. Phys. **96,** 8986 (1992).
[10] A. J. Coleman, Rev. Mod. Phys. **35,** 668 (1963).
[11] R. C. Raffenetti and K. Ruedenberg, Int. J. Quantum Chem. Symp. **3,** 625 (1970). The authors of the present paper became aware of this work *after* rederiving the formulas and developing the program used here. Even the name "Generalized Euler" angles proved to be identical.
[12] NAG Fortran Library Mark 12, Numerical Algorithm Group, Oxford 1986.
[13] R. O. Esquivel and A. V. Bunge, Int. J. Quantum Chem. **32,** 295 (1987).
[14] R. Benesch, S. R. Singh, and V. H. Smith, Jr., Chem. Pys. Lett. **10,** 151 (1971).
[15] E. Clementi and C. Roetti, Atom. Data Nucl. Data Tables **14,** 177 (1974).
[16] E. Clementi, IBM J. Res. Develop. **9,** Supplement (1965).
[17] T. Kato, Commun. Pure Appl. Math. **10,** 151 (1957).
[18] R. Benesch and V. H. Smith, Jr., Density Matrix Methods in X-Ray Scattering and Momentum Space Calculations, in: Wave Mechanics – The First Fifty Years (W. C. Price, S. S. Chissick, and T. Ravensdale, eds.), Butterworths Publishing Company, London 1973, pp. 357–377.
[19] W. L. Clinton and L. J. Massa, Int. J. Quantum Chem. Symp. **6,** 519 (1972).
[20] A. J. Thakkar, A. M. Simas, and V. H. Smith, Jr., Chem. Phys. **63,** 175 (1981).
[21] H. Schmider and V. H. Smith, Jr., to be published.
[22] A. J. Thakkar, A. C. Tanner, and V. H. Smith, Jr., in: Density Matrices and Density Functionals (R. Erdahl and V. H. Smith, Jr., eds.), D. Reidel Publishing Company 1987, p. 327. It is important not to confuse these coordinates with the intracular and extracular coordinates employed in treatments of pair densities (see e.g. A. J. Thakkar, ibid., p. 553). The latter denote distance and position of two *different* particles, whereas the former refer to two different positions of the same electron.
[23] A. V. Bunge and R. O. Esquivel, Phys. Rev. A **34,** 853 (1986).
[24] J. E. Harriman, Phys. Rev. A **34,** 29 (1986).
[25] W. H. E. Schwarz and B. Müller, Chem. Phys. Lett. **166,** 621 (1990).
[26] J. E. Harriman, Proceedings of the Sagamore X Conference, Z. Naturforsch. **48a,** 203 (1993).
[27] Investigations of the influence of experimental errors are presently carried out in our laboratories, using real experimental data as well as theoretical ones with artificial noise.
[28] H. Schmider, V. H. Smith, Jr., and W. Weyrich, Proceedings of the Sagamore X Conference, Z. Naturforsch. **48a,** 221 (1993).